



Ultra-deep hydrodesulfurization on MoS₂ and Co_{0.1}MoS₂: Intrinsic vs. environmental factors

Teh C. Ho^{*}, Jonathan M. McConnachie

Corporate Strategic Research Labs., ExxonMobil Research and Engineering Co., Annandale, NJ 08801, United States

ARTICLE INFO

Article history:

Received 16 June 2010

Revised 1 October 2010

Accepted 25 October 2010

Available online 26 November 2010

Keywords:

Deep hydrodesulfurization

Hydrodenitrogenation

Organonitrogen inhibition

Hydrogenation

Hydrogenolysis

Volcano plot

Hydrogenation index

ABSTRACT

A hydrogenation index (HI), measured in the hydrodesulfurization (HDS) of dibenzothiophene (DBT), is used to estimate the intrinsic hydrogenation selectivities of MoS₂, Co_{0.1}MoS₂, and two supported HDS catalysts. The HI and catalyst activity for desulfurizing 4,6-diethyl-DBT follow the same trend: MoS₂ >> Co_{0.1}MoS₂ >> supported catalysts. For desulfurizing a petroleum fraction rich in 4,6-alkyl-DBTs and 4-alkyl-DBTs, the activity decreases as follows: Co_{0.1}MoS₂ > supported catalysts >> MoS₂. These results introduce an apparent conundrum: MoS₂ has such a high hydrogenation power and activity for desulfurizing 4,6-diethyl-DBT, why does it perform poorly in real-feed tests? This conundrum is resolved by showing that an ultra-deep HDS catalyst requires an optimum balance between an intrinsic factor (hydrogenation function) and an environmental factor (tolerance of organonitrogen). Incorporating Co into MoS₂ lowers the hydrogenation function of MoS₂ and hence improves tolerance of organonitrogen. This conclusion corroborates the prediction of an early modeling study.

© 2010 Elsevier Inc. All rights reserved.

1. Introduction

Producing low-emissions transportation fuels is one of the highest priorities for the petroleum industry. Hydrodesulfurization (HDS) [1,2] has been and will continue to be the most cost-effective technology for reducing the sulfur content of motor fuels in the coming decades. More than 10 years ago, diesel sulfur specifications were between 350 and 500 wppm in many countries. Refiners could meet such specifications by desulfurizing the majority of dibenzothiophene (DBT) and some of its alkyl derivatives in middle distillates (200–370° C boiling range; diesel, jet fuel, heating oil, etc.). However, today's 10–15 wppm specifications in a growing number of countries require desulfurization of sterically hindered alkyldibenzothiophenes. Such hindered sulfur species comprise 4-alkyl- and 4,6-alkyl-DBTs, the HDS of which is rather slow over conventional Al₂O₃-supported metal sulfide catalysts. Great strides have been made to discover and develop new or much improved catalysts for ultra-deep HDS of middle distillates, a term synonymous with the HDS of sterically hindered DBTs.

Transition metal sulfides (TMS) are the workhorse catalysts for the HDS of a multitude of refinery feedstocks. The most widely used components in TMS catalysts are molybdenum sulfide

promoted by Co or Ni [1,2]. The HDS of DBT on TMS catalysts produces two primary hydrocarbon products: biphenyl (BP) and cyclohexylbenzene (CHB). The former reflects the catalyst's hydrogenolysis (HYL) function for direct C–S bond cleavage. The latter signifies the catalyst's hydrogenation (HYA) function to effect ring hydrogenation followed by C–S bond cleavage [3,4].

The nanostructures of TMS catalysts are exceedingly difficult to characterize because they are in a poorly crystalline and highly disordered state. The active sites are generally believed to be sulfur vacancies associated with Mo (or W) cations and SH[−]/S^{2−} groups on the edges and corners of MoS₂ (WS₂) crystallites [1,2]. Some of the Mo cations are substituted by the promoter metal Co or Ni. Many possible structural configurations with varying degrees of coordinative unsaturation can exist, each having its own activity/selectivity for HYA and HYL. Recently, nonvacancy sites have been identified; they are metallic brim sites with remarkable hydrogenation function [5,6]. For simplicity, it is customary to lump various active sites into two types: HYA and HYL. Each type is a collection of different sites that presumably share some common characteristics.

It is generally believed that the presence of Co decreases the strength of the metal–S bond and increases the electron density on the sulfur atoms [7–10]. In the latter case, the basicity of surface S^{2−} species is strengthened, which may facilitate C–S bond cleavage [11]. The Co used in conventional supported catalysts indeed enhances the selectivity toward HYL [4,12]. The incorporation of Co/Ni also appears to increase the rate of hydrogen activation

^{*} Corresponding author.

E-mail address: teh.c.ho@exxonmobil.com (T.C. Ho).

and adsorption, even though there is little change in the total amount of adsorbed hydrogen [13,14].

Kinetic modeling of the HDS of 4,6-diethyldibenzothiophene (46DEDBT) [15] and of DBT [16] on a sulfided $\text{Co}_x\text{Mo}/\text{Al}_2\text{O}_3\text{-SiO}_2$ ($x > 0.3$) catalyst indicated that HYL sites are more resilient to inhibition by 3-ethylcarbazole (3ECBZ) than HYA sites [16]. This finding, based on model-compound experiments, led to the supposition that the increased HYL selectivity via Co promotion may actually help mitigate organonitrogen inhibition. The present study provides corroborating evidence for this supposition based on results obtained from combined real-feed and model-compound experiments. To this end, we develop a method of determining a catalyst descriptor called hydrogenation index (HI) that estimates a TMS catalyst's selectivity toward hydrogenation. We measure HIs and HDS activities of five MoS_2 -based catalysts. Two of them are unsupported MoS_2 and $\text{Co}_{0.1}\text{MoS}_2$ prepared from the same precursor. For the $\text{Co}_{0.1}\text{MoS}_2$ catalyst, the small amount of Co was selectively incorporated into MoS_2 's edge planes with minimum disturbances. The baseline data were obtained with three commercial supported metal sulfide catalysts, $\text{Co}_x\text{Mo}/\text{Al}_2\text{O}_3\text{-SiO}_2$, $\text{Ni}_y\text{Mo}/\text{Al}_2\text{O}_3$ ($y > 0.3$), and $\text{Co}_z\text{Mo}/\text{Al}_2\text{O}_3$ ($z > 0.3$). The catalyst activity and selectivity tests were performed with a prehydrotreated middle distillate, DBT, and 46DEDBT. The results, together with literature model-compound and real-feed data, show that ultra-deep HDS catalysts require a proper balance between hydrogenation function and tolerance of organonitrogen inhibition.

2. Experimental

2.1. Catalysts

A high-surface-area ($143 \text{ m}^2/\text{g}$) unsupported molybdenum sulfide sample was synthesized from $(\text{NH}_4)_2\text{MoS}_3 \cdot 1.5\text{H}_2\text{O}$ {molybdate(2-), tris[μ -(disulfur- κ_{S_1} , κ_{S_2} ; κ_{S_1} , κ_{S_2})]tris(dithio)- μ_3 -thioxo-tri-, triangulo, ammonium (1:2), hydrate} by heating with a ramp rate of $25^\circ\text{C}/\text{min}$ to 400°C and holding for 1 h under a nitrogen flow rate of $200 \text{ cc}/\text{min}$ [17]. The molybdenum sulfide sample as synthesized has a stoichiometry of $\text{MoS}_{2.7}$. When exposed to the hydrogen atmosphere in the reactor, it loses excess sulfur, resulting in the stoichiometry of MoS_2 . Such a reduction leads to a weight loss of about 12%. The cobalt was added to the molybdenum sulfide sample at room temperature via the direct low-valent promotion (LVP) method [18]. This method makes effective use of the metals; the amount of Co added is sufficient to “decorate” all the edge planes of MoS_2 particles.

Specifically, the LVP preparation proceeded as follows. In a 250-mL Schlenk flask under nitrogen, 1.3 g of $\text{Co}_2(\text{CO})_8$ was dissolved in 43 mL anhydrous hexane. Twelve grams of the high-surface-area unsupported molybdenum sulfide was added and the mixture stirred for 20 h. The solid product was filtered off, washed with anhydrous hexane until the wash hexane was colorless, and dried under vacuum. Both solid samples, being pyrophoric, were stored in a glove box under nitrogen prior to activity tests. Elemental analysis of the Co-promoted molybdenum sulfide after HDS activity tests indicated a stoichiometry of $\text{Co}_{0.1}\text{MoS}_2$. The MoS_2 and $\text{Co}_{0.1}\text{MoS}_2$ catalysts have approximately the same reactor packing density ($\sim 1 \text{ g}/\text{cc}$).

The three commercial $\text{Co}_x\text{Mo}/\text{Al}_2\text{O}_3\text{-SiO}_2$, $\text{Ni}_y\text{Mo}/\text{Al}_2\text{O}_3$, and $\text{Co}_z\text{Mo}/\text{Al}_2\text{O}_3$ catalysts are designated as A–C, respectively. Catalysts A and B were pre-sulfided at 400°C for 2 h at atmospheric pressure with a 10% H_2S -in- H_2 mixture. Catalyst C was liquid sulfided with dimethyl disulfide. All catalysts were in the form of 20/40-mesh granules before being charged to the reactor.

2.2. Catalyst activity and selectivity tests

2.2.1. Model compounds

Model-compound HDS experiments were carried out in a unit consisting of two parallel cocurrent fixed-bed reactors (3/8-in. OD 316 stainless steel pipe) in a common heated box. The reactors were operated isothermally in up-flow mode to avoid incomplete catalyst wetting and bypassing. Axial dispersion was minimized through dilution with fine inert particles. The catalyst bed was in the central zone of the reactor, which was packed with inert materials in the fore and aft zones. The reaction conditions were 265°C , 1.83 MPa hydrogen pressure, and 116 cc H_2/cc liquid feed. The liquid weight hourly space velocity (WHSV) was varied to obtain different HDS levels.

The sulfur compounds used were DBT and 46DEDBT. Two liquid feed solutions were prepared. With dodecane as the solvent, Feeds I and II contained 1.5 wt.% DBT and 0.8 wt.% 46DEDBT, respectively. Over the conditions tested, the dominant products from the HDS of DBT are BP, CHB, and H_2S . In the kinetic analysis to follow, the trace amounts of tetrahydrodibenzothiophene (THDBT), bicyclohexyl (BCH), and benzylcyclopentane (BCP) were not considered. The analyses of reaction products were more involved for the HDS of 46DEDBT. The following products were identified and quantified: diethylcyclohexylbenzenes (C4CHB), diethylbiphenyls (C4BP), ethylcyclohexylbenzenes (C2CHB), ethylbiphenyls (C2BP), ethylbenzenes, and ethylcyclohexanes. Each of these products has many isomers. Other minor products include diethylbicyclohexyl, ethylbicyclohexyl, biphenyl, and cyclohexylbenzene.

2.2.2. Real feed

Real-feed tests were performed for about 10 days in an up-flow, multi-tube reactor unit with a prehydrotreated middle distillate at 329°C , 4.6 MPa H_2 pressure, 2.0 liquid hourly space velocity, and 2000 SCF/B (standard cubic feet/barrel oil feed) hydrogen treat gas rate. The API gravity, sulfur, and nitrogen contents of this feed-stock are 35.9°, 592 wppm, and 100 wppm, respectively. The high API gravity implies a low level of polynuclear aromatics. As will be discussed later, prehydrotreated middle distillates in general have a relatively low level of total sulfur but a disproportionately high concentration of hindered DBTs.

3. Hydrogenation index

In heterogeneous catalysis, it is often useful to conduct standardized model-compound reaction tests for probing certain catalytic functions. The constrained [19] and spaciousness [20] indexes are two such examples for characterizing zeolite catalysts. In this section, we attempt to develop a simple model-compound test for characterizing the intrinsic HYA selectivity of TMS catalysts. By intrinsic, it is meant that the selectivity test is conducted in the absence of any inhibitor such as nitrogen or aromatic compounds. Over supported HDS catalysts, many studies have shown that the HDS of DBT relies primarily on the HYL pathway, while the HDS of hindered DBTs favors strongly the HYA pathway [2–4]. For a given family of TMS catalysts (e.g., MoS_2 -based catalysts), there are no *a priori* reasons why the intrinsic activity for DBT HDS should correlate with that for the HDS of hindered DBTs. It seems plausible, however, that a properly defined hydrogenation index for the HDS of DBT may correlate with catalyst activity for the HDS of hindered DBTs. We pursue this point in what follows.

With the assumption of pseudo-first-order kinetics in an isothermal/isobaric plug flow reactor, a simple way of gauging a catalyst's selectivity for hydrogenation at a given DBT conversion is to measure γ_{DBT} defined as

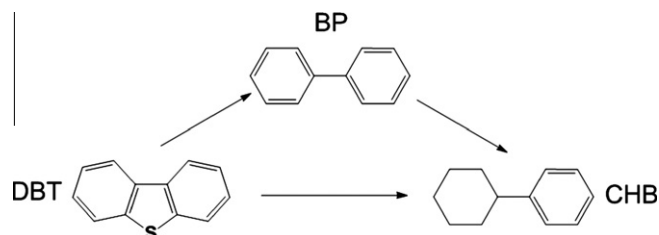


Fig. 1. Triangular reaction network for DBT HDS.

$$\gamma_{\text{DBT}} = \frac{[\text{CHB}]}{[\text{BP}]} \quad (1)$$

Here, [CHB] and [BP] are concentrations (wt.%) of CHB and BP in the liquid effluent, respectively. CHB is much less reactive than BP over TMS catalysts [21,22]. And the hydrogenation of CHB to BCH is unimportant under conditions of practical interest (e.g., due to the need of minimizing hydrogen consumption). With supported CoMo catalysts, $\gamma_{\text{DBT}} \approx \text{constant}$ over a wide range of DBT conversions by varying reaction time, suggesting that DBT HDS is nearly parallel under the conditions used [4,23]. With supported NiMo catalysts, γ_{DBT} has been observed to be an increasing function of DBT conversion [23,24] due to non-negligible hydrogenation of BP to CHB. Unsupported TMS catalysts are known to be more hydrogenative than Al_2O_3 -supported TMS catalysts [25–27]. In this and similar cases, the hydrogenation of BP to CHB plays a significant role, as will be seen later. Fig. 1 shows that the disappearance of DBT in general follows a triangular pathway.

Before proceeding further, we remark that one can define a similar hydrogenation selectivity for the HDS of 46DEDDBT as $\gamma_{\text{DEDBT}} = [\text{C4CHB}]/[\text{C4BP}]$. For perspective, Catalyst A gives a $\gamma_{\text{DBT}} \sim 0.3$, versus $\gamma_{\text{DEDBT}} \sim 5.5$ [28]. The high γ_{DEDBT} , as alluded to earlier, indicates that the HDS of hindered DBTs is a hydrogen intensive process requiring a strong HYA functionality. As an aside, here for simplicity, we do not include C2BP and C2CHB in HYA selectivity calculations.

In commercial deep HDS processes, no significant HDS of hindered DBTs is expected until the bulk of DBT is almost completely desulfurized (more on this in Section 6.1). To be relevant to the HDS of hindered DBTs, a hydrogenation index (HI) measured from DBT HDS experiments should reflect the maximum hydrogenation power of the TMS catalyst in question. It is thus sensible to measure γ_{DBT} at high DBT conversions (say, 80–99%). Such experiments should be carried out by varying reaction (or space) time at constant temperature, pressure, and hydrogen treat gas rate. The HI is defined as follows

$$\text{HI} = \text{maximum } \gamma_{\text{DBT}} \quad (2)$$

We next see whether the thus-obtained HI can at least provide a qualitative ranking of catalysts' activities for the HDS of 46DEDDBT, a severely hindered DBT.

4. Model-compound test results

Fig. 2 plots γ_{DBT} vs. percent HDS for MoS_2 , $\text{Co}_{0.1}\text{MoS}_2$, and Catalyst A in HDS tests with DBT. The hydrogenation function of the unsupported MoS_2 is so strong that its γ_{DBT} is far higher than those observed with other catalysts including the highly hydrogenative $\text{Co}_{0.1}\text{MoS}_2$. Moreover, MoS_2 's γ_{DBT} is an increasing function of DBT conversion and asymptotically reaches a plateau when the HDS level exceeds 95%.

The HI defined in Eq. (2) is taken as a measure of a catalyst's HYA function relative to its HYL function. As Fig. 2 indicates, the MoS_2 catalyst gives an HI of about seven, compared to $\text{HI} \approx 0.3$

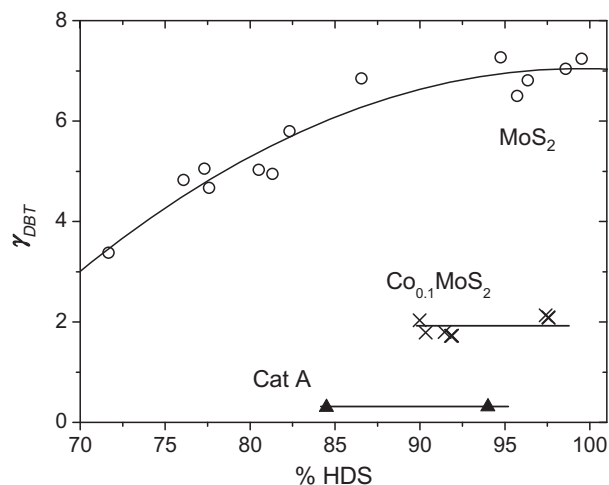


Fig. 2. γ_{DBT} vs. percent DBT HDS for MoS_2 , $\text{Co}_{0.1}\text{MoS}_2$, and Catalyst A; 265 °C, 1.83 MPa H_2 pressure, and 116 cc H_2 /cc liquid feed; liquid feed contains 1.5 wt.% DBT in dodecane.

for Catalyst A. This unusually high HI for MoS_2 counters the common notion that the HDS of DBT proceeds predominantly via the HYL route. It also demonstrates that the HYA and HYL functionalities can be independently tuned.

As can be seen from Fig. 2, the incorporation of a small amount of Co into MoS_2 substantially reduces the HYA selectivity, resulting in a decrease in HI from seven to two. Notwithstanding this, an HI of two is still remarkably high relative to that for Catalyst A whose $\text{HI} \ll 1$. Thus, unlike supported catalysts, MoS_2 and $\text{Co}_{0.1}\text{MoS}_2$ both rely primarily on the HYA pathway even in the HDS of DBT.

Table 1 compares the gravimetric activities of $\text{Co}_{0.1}\text{MoS}_2$ and MoS_2 for the HDS of DBT in terms of k_{DBT} , the pseudo-first-order rate constant (cc liquid feed/g cat/h based on catalyst's pre-reduction weight). As expected, $\text{Co}_{0.1}\text{MoS}_2$ is more active than MoS_2 for desulfurizing DBT. This is also in line with the prevailing view that Co as a promoter boosts the overall HDS activity by preferentially speeding up the HYL rate, resulting in a lower HI value.

Fig. 3 shows that HI correlates with catalyst's activity for desulfurizing 46DEDDBT. Here, the activity, represented by $k_{46\text{DEDDBT}}$, is calculated as the gravimetric pseudo-first-order rate constant. One sees that $k_{46\text{DEDDBT}}$ and HI both follow the same trend: $\text{MoS}_2 \gg \text{Co}_{0.1}\text{MoS}_2 \gg \text{Ni}_y\text{Mo}/\text{Al}_2\text{O}_3 > \text{Co}_x\text{Mo}/\text{Al}_2\text{O}_3\text{--SiO}_2$. This result is not surprising in that unsupported catalysts are in general more HYA-selective than Al_2O_3 -supported catalysts [25–27]. Fig. 3 (inset) also shows the expected trend: Catalyst B has a higher HI than Catalyst A, 1.09 vs. 0.33. Moreover, it indicates that the HIs of commercial supported CoMo and NiMo catalysts are clustered within a narrow range. The HI of MoS_2 is an order of magnitude higher than those of supported catalysts. Hence, the inclusion of unsupported catalysts significantly expands the feasible range of HI.

Fig. 4 summarizes remarkable activity reversal behaviors. The incorporation of a small amount of Co into MoS_2 increases the HDS rate of DBT but decreases the HDS rate of 46DEDDBT. Put differently, Co can promote or demote the HDS activity of MoS_2 ,

Table 1

Pseudo-first-order gravimetric rate constants and HIs for MoS_2 and $\text{Co}_{0.1}\text{MoS}_2$ in the HDS of DBT.

	MoS_2	$\text{Co}_{0.1}\text{MoS}_2$
k_{DBT}	6.2	10.0
HI	7	2

k_{DBT} : cc liquid feed/g cat/s.

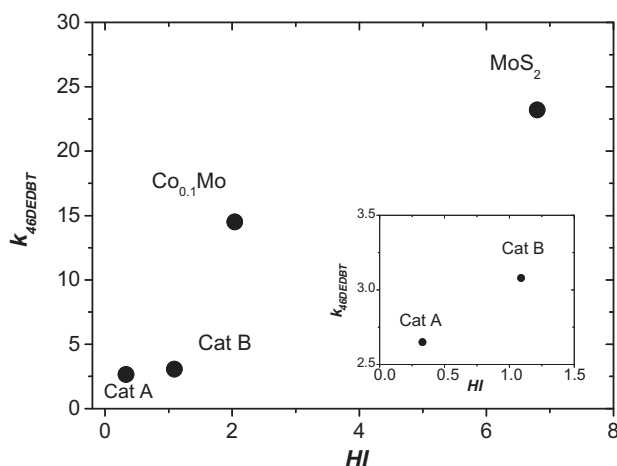


Fig. 3. Pseudo-first-order rate constants $k_{46DEDBT}$ vs. HI; MoS_2 , $\text{Co}_{0.1}\text{MoS}_2$, Catalysts A and B; 265 °C, 1.83 MPa H_2 pressure, and 116 cc H_2 /cc liquid feed; liquid feed contains 0.8 wt.% 46DEDBT in dodecane.

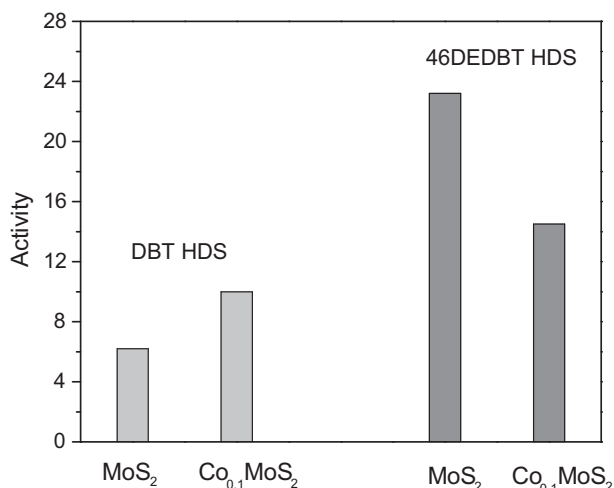


Fig. 4. Comparison of pseudo-first-order rate constants for MoS_2 (HI = 7) and $\text{Co}_{0.1}\text{MoS}_2$ (HI = 2) in the HDS of DBT and 4,6-diethyl-DBT; two different feeds, one containing 1.5 wt.% DBT and the other 0.8 wt.% 46DEDBT; 265 °C, 1.83 MPa H_2 pressure, and 116 cc H_2 /cc liquid feed.

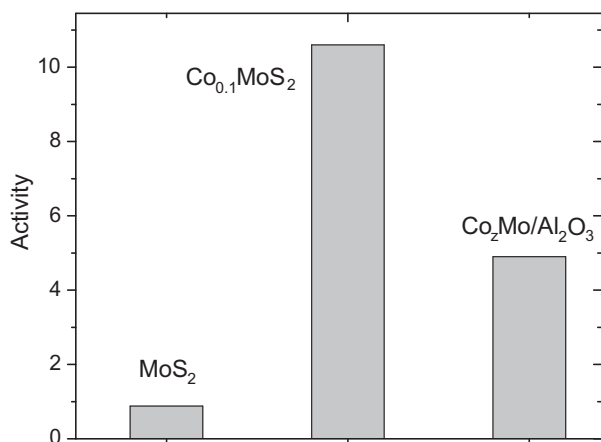


Fig. 5. Pseudo-first-order rate constants for MoS_2 , $\text{Co}_{0.1}\text{MoS}_2$, and Catalyst C ($\text{Co}_2\text{Mo}/\text{Al}_2\text{O}_3$, $z > 0.3$); prehydrotreated middle distillate; 329.4 °C, 4.6 MPa H_2 pressure, 2.0 LHSV, and 2000 SCF/B H_2 treat gas rate.

depending on the structure of the sulfur species to be desulfurized. In the same vein, 46DEDBT can be more or less refractory than DBT, depending on the catalyst. Due to their high hydrogenation functions, both MoS_2 and $\text{Co}_{0.1}\text{MoS}_2$ desulfurize 46DEDBT faster than they desulfurize DBT.

5. Real-feed test results

Catalyst C has an HI value comparable to that of Catalyst A. After an 8-day activity line-out period with the prehydrotreated distillate, the percents HDS obtained with MoS_2 , $\text{Co}_{0.1}\text{MoS}_2$, and Catalyst C are 35, 99.5, and 91, respectively. Fig. 5 compares the volumetric HDS first-order rate constants for these catalysts. Contrary to the model-compound results, here MoS_2 is far less active than $\text{Co}_{0.1}\text{MoS}_2$. It is also less active than Catalyst C. At the condition tested, $\text{Co}_{0.1}\text{MoS}_2$ reaches the ultra-deep-HDS regime of 3 wppm product sulfur and is much more active than Catalyst C.

6. Discussions

The forgoing results say that while the highly HYA-selective MoS_2 is much more active than $\text{Co}_{0.1}\text{MoS}_2$ in the HDS of 46DEDBT, it is far less active in the HDS of a petroleum distillate rich in hindered DBTs. This introduces an apparent conundrum: If MoS_2 has such a high HYA power and activity for desulfurizing 46DEDBT, why is that it performs so poorly in the HDS of the prehydrotreated distillate? It is unlikely that the low activity of MoS_2 in the real-feed test is caused by sintering because the catalyst's activity increased during the activity line-out period in both real-feed and model-compound tests. Also, the MoS_2 catalyst maintained its activity for 500 h in tests with DBT and 46DEDBT. To help resolve the conundrum, we first give a qualitative recapitulation of HDS property–reactivity correlations for middle distillates [29,30].

6.1. Real-feed HDS environment

We consider a hypothetical raw middle distillate containing 1 wt.% sulfur. The relative distributions of different sulfur and nitrogen heterocyclic structures in this distillate are characterized by two parameters α and β . The former measures the concentration of hindered DBTs relative to that of total DBTs. The latter measures the concentration of five-membered ring nitrogen heterocycles relative to that of total nitrogen heterocycles. Thus,

$$\alpha = \frac{[\text{4-alkyl-DBTs}] + [\text{4,6-alkyl-DBTs}]}{[\text{all DBTs}]} \leq 1 \quad (3)$$

$$\beta = \frac{[\text{5-membered N}]}{[\text{5-membered N}] + [\text{6-membered N}]} \leq 1 \quad (4)$$

where N stands for nitrogen heterocycles.

For ease of discussion, let us break the HDS process into two steps. In the first step, the sulfur is reduced to, say, 300 wppm. The resulting low-sulfur (prehydrotreated) stream is further desulfurized in the second step to produce an ultra low-sulfur diesel containing 10 wppm sulfur. Thus, the extents of HDS in both steps are deep (~97% HDS), but the reaction environments are very different, as explained below.

The HDS in the first step is performed in a high-sulfur environment with relatively low α , β , and API gravity. In this case, of 24 feed properties and their linear combinations, the API gravity of the distillate is by far the most influential property dictating the distillate's HDS reactivity [29]. This implies that here the HDS is dominated by the inhibiting effect of polynuclear aromatics due to their heaviness/size [31] and high concentration.

After the treatment in the first step, the concentrations of reactive sulfur species (e.g., non-hindered DBTs) and polynuclear aromatics are significantly reduced. The concentration of highly basic six-membered ring nitrogen heterocycles (e.g., alkylpyridines, alkylquinolines) is also diminished due to preferential chemisorption. As a result, the residual nitrogen species are mostly carbazole and its alkyl derivatives [26,32,33].

The HDS in the second step is performed in a low-sulfur environment in which α , β , and API gravity are all relatively high. For instance, the prehydrotreated feed used in this study has an $\alpha \sim 0.9$. Of 24 feed properties and their linear combinations, the concentration of nitrogen in the feed was found to be the primary indicator of HDS reactivity [30]. This implies that the extent of HDS is primarily governed by the inhibiting effect of nitrogen species. Indeed, in the HDS of prehydrotreated oils, van Looij et al. observed a profound nitrogen inhibition effect with feed nitrogen as low as 30 ppm [34]. Note that partially hydrogenated nitrogen species generated in the first step can be highly inhibiting to sulfur removal in the second step ([33] and references therein). Results from controlled real-feed experiments have shown that nitrogen species are much more potent in inhibiting hindered DBTs than in inhibiting unhindered DBTs [35,36]. One reason for the strong nitrogen inhibiting effect is that the desorption of heterocyclic nitrogen species is much slower than adsorption [37].

Summarizing, the limiting environmental factor changes in going from the high-sulfur regime to the low-sulfur regime. Initially, polynuclear aromatics are the dominant inhibitor. As the desulfurization gets deeper, nitrogen heterocycles emerge as the dominant inhibitor. In fact, HDN is limited by self-inhibition [33].

6.2. Nitrogen inhibition in the HDS of model-compounds

We now show that the forgoing real-feed results are consistent with those observed in model-compound HDS experiments using 3ECBZ as the inhibitor. DBT and 46DEDBT were used as the probe molecules for the first- and second-step HDS, respectively [15,16,28]. Fig. 6 shows the inhibiting effect of feed nitrogen content over Catalyst A. As can be seen, the HDS of 46DEDBT decreases precipitously upon addition of 5 wppm nitrogen atom to the feed. In contrast, the inhibiting effect on the HDS of DBT is quite moderate; the extent of inhibition at 80 wppm feed nitrogen is far lower

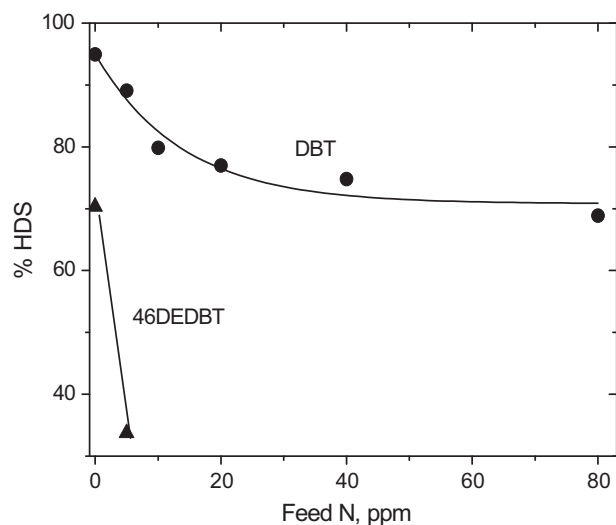


Fig. 6. Effect of feed nitrogen concentration on the HDS of DBT and 46DEDBT on Catalyst A; two different feeds, one containing 1.5 wt.% DBT and the other 0.8 wt.% 46DEDBT; 265 °C, 1.83 MPa H₂ pressure, and 116 cc H₂/cc liquid feed.

than that with 46DEDBT HDS at 5 wppm nitrogen. Thus, 46DEDBT HDS is extremely sensitive to 3ECBZ, whereas DBT HDS is not. In either case, the presence of 3ECBZ results in a sharp decrease in γ_{DBT} and γ_{DEDBT} , implying that HYA sites are more vulnerable to nitrogen inhibition than HYL sites [16,28]. In fact, it has been noted that while nitrogen inhibition on HYL sites is reversible, it is only partially reversible on HYA sites [38]. In a nut shell, a high HI catalyst is more sensitive to nitrogen inhibition than a low HI catalyst.

6.3. Resilience to nitrogen inhibition: hydrogenation vs. hydrogenolysis sites

A quantitative analysis of the relative resistances of HYA and HYL sites to nitrogen inhibition was performed through modeling of transient experiments using DBT and 3ECBZ as probe molecules over Catalyst A [16]. The inhibition intensity on the catalyst can be quantified by a dimensionless parameter defined as

$$g = \frac{k_n N_f}{k_{\text{HDN}}} \quad (5)$$

where k_n , N_f , and k_{HDN} are the organonitrogen adsorption rate constant, feed nitrogen concentration, and the surface HDN rate constant, respectively. Eq. (5) says that g is nothing but the ratio of organonitrogen adsorption rate to surface HDN rate. With the subscripts HYA and HYL denoting the hydrogenation and hydrogenolysis sites, it was found that $k_{n,\text{HYL}} < k_{n,\text{HYA}}$ and $k_{\text{HDN},\text{HYL}} > k_{\text{HDN},\text{HYA}}$. For Catalyst A, the result was that [16]

$$\frac{g_{\text{HYA}}}{g_{\text{HYL}}} = 3.8 \quad (6)$$

That is, the inhibition severity for HYA sites is about four times that for HYL sites. It is no wonder that the majority of HDS is actually carried out on HYL sites in the presence of 3ECBZ [16].

6.4. Intrinsic vs. environmental factors

The focus of the present study is on the ultra-deep HDS regime (e.g., HDS of prehydrotreated feedstocks). It transpires from the foregoing discussions that there are two determining factors in this regime. One is the HI, which is an intrinsic catalyst property for activating/desulfurizing sterically hindered DBTs. The other is the environment factor referring to organonitrogen inhibition. From the prospective of HI, the catalyst ranking order is

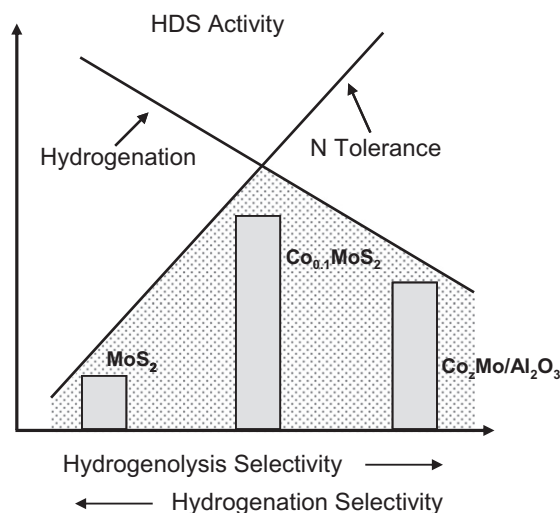


Fig. 7. A “volcano” plot showing that the high activity of Co_{0.1}MoS₂ represents a proper balance between hydrogenation function and tolerance of organonitrogen.

$\text{MoS}_2 > \text{Co}_{0.1}\text{MoS}_2 > \text{Catalyst C}$. On the other hand, from the prospective of nitrogen tolerance, the ranking order is reversed: Catalyst C $> \text{Co}_{0.1}\text{MoS}_2 > \text{MoS}_2$. The high nitrogen tolerance of Catalyst C is related to its low hydrogenation function.

The high activity of $\text{Co}_{0.1}\text{MoS}_2$ observed in the real-feed tests (Fig. 5) arises mainly from a proper balance between the HI and nitrogen tolerance. Conceptually, this trade-off is shown in Fig. 7 as a “volcano” plot for real-world ultra-deep HDS. On the right-hand side, the $\text{Co}_2\text{Mo}/\text{Al}_2\text{O}_3$ catalyst does not have sufficient hydrogenation power to activate and desulfurize hindered DBTs. On the left-hand side, the plentiful high-power hydrogenation sites on MoS_2 become incapacitated upon adsorption of nitrogen species. The incorporation of a small amount of Co into MoS_2 lowers the hydrogenation function to an intermediate level, thereby enhancing the resilience to nitrogen inhibition. Fig. 7 appears to resolve the aforementioned model-compound-vs.-real-feed conundrum. It also explains two real-feed results. One is that a $\text{CoMo}/\text{Al}_2\text{O}_3$ (low HI) catalyst outperforms $\text{NiMo}/\text{Al}_2\text{O}_3$ (high HI) in the HDS of an oil fraction rich in hindered DBTs and carbazoles [39]. The other has to do with optimization of a stacked bed containing two different catalysts. The preferred stacking order is to put a low HI catalyst upstream of a high HI catalyst [26,40].

7. Concluding remarks

Among all sulfur-containing heterocyclic species in middle distillates, DBT is a unique probe molecule allowing for a simple, clear-cut distinction between the hydrogenation and hydrogenolysis functions (pathways). For a given family of catalysts, the HI defined in this work can be used as a rough indicator of the strength of a catalyst's intrinsic hydrogenation functionality. The HI correlates with the intrinsic activity for removing sulfur from 46DEDBT. As such, it may have a bearing on hydrodenitrogenation and hydrodearomatization as well. Model-compound testing and evaluation of hydroprocessing exploratory catalysts must be conducted in an adsorption competitive environment. This is so because an active ultra-deep HDS catalyst requires a delicate balance between the hydrogenation function and tolerance of organonitrogen inhibition. Cobalt as a promoter plays an important role in helping MoS_2 -based catalysts combating organonitrogen inhibition. The present study lends support to an early supposition [16] that the addition of Co to MoS_2 dampens the nitrogen inhibiting effect on HDS owing to the enhanced hydrogenolysis functionality.

References

- [1] H. Topsøe, B.S. Clausen, F.E. Massoth, *Hydrotreating Catalysis*, Springer-Verlag, 1996.
- [2] T. Kabe, A. Ishihara, W. Qian, *Hydrodesulfurization and Hydrodenitrogenation*, Wiley-VCH, New York, 1999.
- [3] M.J. Girgis, B.C. Gates, *Ind. Eng. Chem. Res.* 30 (1991) 2021.
- [4] M. Egorova, R. Prins, *J. Catal.* 225 (2004) 417.
- [5] J.V. Lauritsen, S. Helveg, E. Lægsgaard, I. Stensgaard, B.S. Clausen, H. Topsøe, F. Besenbacher, *J. Catal.* 197 (2001) 1.
- [6] J.V. Lauritsen, M. Nyberg, J.K. Nørskov, B.S. Clausen, H. Topsøe, E. Lægsgaard, F. Besenbacher, *J. Catal.* 224 (2004) 94.
- [7] R.R. Chianelli, *Catal. Rev. Sci. Eng.* 26 (1984) 361.
- [8] H. Topsøe, B.S. Clausen, N.Y. Topsøe, E. Pedersen, W. Niemann, A. Müller, H. Bögge, B. Lengeler, *J. Chem. Soc., Faraday Trans. 1* 83 (1987) 2157.
- [9] H. Topsøe, B.S. Clausen, F.E. Massoth, in: J.R. Anderson, M. Boudard (Eds.), *Catalysis, Science and Technology*, vol. 11, Springer-Verlag, Berlin, 1996.
- [10] L.S. Byskov, B. Hammer, J.K. Nørskov, B.S. Clausen, H. Topsøe, *Catal. Lett.* 47 (1997) 177–182.
- [11] J. Mijoin, V. Thévenin, N. Garcia Aguirre, H. Yuze, J. Wang, W.Z. Li, G. Pérot, J.L. Lemberston, *Appl. Catal. A* 180 (1999) 95.
- [12] F. Bataille, J. Lemberston, P. Michaud, G. Pérot, M. Vrinat, M. Lemaire, E. Schulz, M. Breyse, S. Kasztelan, *J. Catal.* 191 (2000) 409.
- [13] N.M. Rodriguez, R.T.K. Baker, *J. Catal.* 140 (1993) 287.
- [14] E.J.M. Hensen, G.M.H. Lardinois, V.H.J. de Beer, J.A.R. van Veen, R.A. van Santen, *J. Catal.* 187 (1999) 95.
- [15] T.C. Ho, D. Nguyen, *J. Catal.* 222 (2004) 450.
- [16] T.C. Ho, L. Qiao, *J. Catal.* 269 (2010) 291.
- [17] A.W. Naumann, E.M. Thorsteinson, in: H.F. Barry, P.C.H. Mitchell (Eds.), *Proceedings of the Climax Fourth International Conference on the Chemistry and Uses of Molybdenum*, Climax Molybdenum Company, Ann Arbor Michigan, 1982, pp. 313–318.
- [18] T.R. Halbert, T.C. Ho, E.I. Stiefel, R.R. Chianelli, M. Daage, *J. Catal.* 130 (1991) 116.
- [19] V.J. Frillette, W.O. Haag, R.M. Lago, *J. Catal.* 67 (1991) 218.
- [20] J. Weitkamp, S. Ernst, R. Kumar, *Appl. Catal.* 27 (1986) 207.
- [21] G.H. Singhai, R.L. Espino, J.E. Sobel, G.A. Huff, *J. Catal.* 67 (1981) 457.
- [22] C. Aubert, R. Durand, P. Geneste, C. Moreau, *J. Catal.* 112 (1988) 12.
- [23] M.V. Landau, D. Berger, M. Herskowitz, *J. Catal.* 159 (1996) 236.
- [24] T.C. Ho, J.E. Sobel, *J. Catal.* 128 (1991) 581.
- [25] N. Hermann, M. Brorson, H. Topsøe, *Catal. Lett.* 65 (2000) 169.
- [26] T.C. Ho, *Catal. Today* 98 (2004) 3.
- [27] T.C. Ho, *Catal. Today* 130 (2008) 206.
- [28] T.C. Ho, *J. Catal.* 219 (2003) 442.
- [29] T.C. Ho, *Appl. Catal., A: Gen.* 244 (2003) 115.
- [30] T.C. Ho, G.E. Markley, *Appl. Catal., A: Gen.* 267 (1–2) (2004) 245.
- [31] S. Korre, M. Neurock, M.T. Klein, R.J. Quann, *Chem. Eng. Sci.* 49 (1994) 4191.
- [32] C.W. Hudson, *US Patent* 4591430, 1986.
- [33] T.C. Ho, *Appl. Catal., A: Gen.* 378 (2010) 52.
- [34] F. van Looij, P. van der Laan, W.H.J. Stork, D.J. Di Camillo, J. Swain, *Appl. Catal., A: Gen.* 170 (1998) 1.
- [35] H. Yang, J. Chen, C. Fairbridge, Y. Briker, Y.J. Zhu, Z. Ring, *Fuel Process. Technol.* 85 (2004) 1415.
- [36] H. Yang, J. Chen, Y. Briker, R. Szynekarczuk, Z. Ring, *Catal. Today* 109 (2005) 16.
- [37] M. Sau, K. Basak, U. Manna, M. Santra, R.P. Verma, *Catal. Today* 109 (2005) 112.
- [38] T.C. Ho, J.E. Sobel, *Catal. Lett.* 99 (2005) 109.
- [39] K.H. Choi, Y. Sano, Y. Korai, I. Mochida, *Appl. Catal., B: Environ.* 53 (2004) 275.
- [40] T.C. Ho, *US Patent* 4902404, 1990.